Pol. J. Environ. Stud. Vol. XX, No. X (XXXX), 1-12
DOI: *10.15244/pjoes/210390* ONLINE PUBLICATION DATE: 2026-01-07

Original Research

Evaluation of Mechanical Properties and Environmental Benefits of Bentonite-Modified Cement-Stabilized Silt

Zhibo Zhang[1, 2], Wei Chen[1, 2], Xiangcai Pan[1, 2], Fanfei Wu[3], Yu Zhou[1, 4], Qiang Tang[1, 2°*]

[1]School of Rail Transportation, Soochow University, Suzhou, 215131, China
[2]Intelligent Urban Rail Engineering Research Center of Jiangsu Province, Suzhou, 215131, China
[3]School of Biology and Basic Medical Sciences, Soochow University, Suzhou, 215123, China
[4]State Key Laboratory of Disaster Prevention & Mitigation of Explosion & Impact, Army Engineering University of PLA, Nanjing, 210007, China

Received: 23 June 2025
Accepted: 7 September 2025

Abstract

In response to the global drive for carbon neutrality, this study investigates whether bentonite can partially replace cement to enhance the mechanical properties and environmental sustainability of cement-stabilized silt. Laboratory tests and field analyses were conducted on waste sludge for subway tunnel engineering. Results show that bentonite significantly improves unconfined compressive strength, with peak performance at an optimal dosage; excessive addition causes strength loss due to swelling and micro-cracks. Bentonite also increases failure strain and reduces brittleness, with the best effect at 9% content. A linear relationship between the deformation modulus (E_{50}) and compressive strength was confirmed. Permeability decreased significantly at 3% bentonite and then stabilized. Strain energy analysis verified improved fracture resistance. Importantly, using bentonite can reduce cement usage by up to 30%, saving about 200,000 kcal of energy per ton of mixture. Field tests further validate its practical effectiveness in subway tunnel applications. Overall, the findings confirm that the study's goal was achieved, demonstrating both structural and environmental benefits, and providing a practical reference for sustainable construction practices.

Keywords: bentonite-silt-cement composites, unconfined compressive strength, soil permeability, energy consumption, carbon emission

*e-mail: tangqiang@suda.edu.cn
Tel.: +86-183-6267-6527
°ORCID iD: 0000-0003-0861-9943

Nomenclature

Parameters	Description
q_u	The unconfined compressive strength of waste sludge with bentonite
q_0	The unconfined compressive strength of waste sludge without bentonite
Δq_u	The absolute difference in strength between bentonite sludge and non-bentonite sludge
E_{50}	50 % deformation modulus
U	The total energy absorbed by the sample
U_e	The elastic strain energy stored in the sample
U_d	The dissipated energy that is responsible for the plastic deformation and crack propagation
E_0	Initial elasticity modulus
E_u	Unloading elastic modulus
v_0	Initial Poisson's ratio
v_u	Unloading Poisson's ratio
σ_1	Major principal stress
σ_3	Confining pressure
ε_1	Axial strain
ε_3	Lateral strain

Introduction

In the context of rapid socio-economic development today, engineering environments are becoming increasingly complex, especially with the presence of silt layers in construction projects, which has garnered widespread attention. This is because silt layers are characterized by low strength, high compressibility, and high permeability [1]. These characteristics can lead to foundation instability, structural settlement, and leakage in engineering applications, posing significant risks to project safety [2]. Therefore, reinforcing and treating silt layers has become a key measure to ensure the stability of engineering projects and extend their lifespan [3]. Currently, adding cement is a common method for reinforcing soft soils, particularly silt layers [4]. Cement is notably effective in enhancing soil bearing capacity, reducing settlement, and preventing water seepage, and thus is widely used in foundation treatment, embankment slope reinforcement, and hydraulic engineering impermeability [5]. However, the large-scale production of cement leads to significant energy consumption and substantial use of non-renewable raw materials, as well as emissions of large amounts of environmental pollutants [6, 7]. In the face of these severe challenges, it has become an industry consensus to integrate the concept of sustainable development and circular economy into soil reinforcement technology [8, 9]. This makes it imperative to find suitable admixtures to partially replace cement, reduce the amount of cement used, and improve the properties of cement soil. The development of such alternatives needs to consider cost-effectiveness, environmental impact, and practical performance in engineering applications to achieve more sustainable and environmentally friendly construction.

In recent years, scholars have made certain progress in the study of modifying cement soil with various admixtures, such as fly ash, lime, slag, silica fume, geopolymer, bio-cement, etc. [8-12]. Fly ash and slag are widely used in practical engineering, showing good impermeability and durability, but they also lead to slower early strength development in cement soil [13]. Using silica fume to replace part of the cement comprehensively enhances the properties of cement soil, but issues of limited production and unstable quality exist [14]. Similarly, geopolymer technology utilizing industrial by-products (e.g., recycled concrete powder, construction and demolition waste, fly ash/slag, etc.) demonstrates superior early strength and reduced carbon footprint, yet faces challenges in controllable setting time for field applications [15]. Parallel studies on microbially induced calcite precipitation (MICP) reveal that urea-hydrolyzing bacteria can enhance strength through bio-cementation, though inhomogeneous distribution remains a critical limitation [16, 17]. Therefore, an increasing number of scholars are researching bentonite-modified cement soil. Trumer et al. [18] calcined the bentonite from the Westerwald region (at 900°C) and used it to replace 30% of cement to prepare calcined bentonite cement. The results showed that calcined bentonite mixed with cement not only has good strength characteristics but also exhibits excellent early strength properties. Tironi et al. [19] used two types of calcined bentonite as active additives to replace 30% of cement to make two types of mortar. The results showed that the compressive strength at the same age did not differ much and was more than 10% lower than that of cement mortar without bentonite. Laidani et al. [20] pointed out that adding 10% bentonite can increase the compressive strength by 16% in 90 days. Huang [21] also showed that adding natural calcium-based bentonite to mortar can significantly increase the mortar's compressive strength, with the maximum value reaching 47.8 MPa. Additionally, Chew et al. [22] found that the permeability of cement-stabilized clay soil increases with the increase of porosity ratio and is logarithmically related to it. Overall, although preliminary results have been achieved in the study of bentonite-modified cement soil's engineering properties, current research on bentonite-modified cement soil often fails to fully consider the special requirements of sludge layers. Therefore, the impact of the characteristics of sludge layers on bentonite-modified cement soil and its mechanism of action still need further in-depth exploration.

This paper adopts a multi-faceted approach to assess the mechanical properties and permeability of bentonite-silt-cement composite materials.

The initial phase of the study focuses on the preparation of composite material samples with different proportions and conducting comprehensive tests on their mechanical and permeability properties. These tests aim to reveal the mechanical response and impermeability characteristics of the materials under different proportional combinations, while exploring the correlation between their structure and properties through microscopic morphological analysis. Further, the study will investigate the impact of curing time on the composite material's failure strain, as well as the interrelationship between the deformation coefficient and compressive strength. This analysis not only helps in understanding the mechanical behavior of the materials but is also significant for guiding the design and use of materials in practical applications. To combine laboratory research findings with actual engineering needs, this study will also conduct field drilling and sampling to validate the practical application effects of different mix proportions in strongly reinforced and weakly reinforced areas. This includes evaluating the mechanical strength and permeability of the reinforcement materials on site, ensuring a close integration of theoretical research and engineering practice. This will contribute to further integrating theoretical research and practical application in this field.

Materials and Methods

Materials

The mud used in the experiment was prepared from a dredging project in a river channel in Nantong City, Jiangsu Province. The mud is brown and in a flowable plastic state. Its basic physical properties are shown in Table 1. The liquid limit and plastic limit of the soil were determined using a combined liquid-plastic limit device, and are 37.71% and 22.06%, respectively.

Bentonite was purchased from Anhui Xinyi Company, appearing as a white solid. The main chemical components are shown in Table 2. The cement used is 42.5-grade ordinary Portland cement.

Experimental Scheme

Before the experiment, a certain amount of sludge is taken and placed in a plastic barrel, soaked with water, stirred evenly, and the water content is measured. Then, based on the target water content of the slurry and the required admixture dosage in Table 3, the masses of additional water, cement, and bentonite are calculated (the cement dosage is the percentage of cement mass to the dry soil mass, the same below). After that, water and admixtures are added to the sludge and stirred evenly, then sealed and left to stand for 24 hours to allow full interaction between the admixtures and soil particles [23]. This paper mainly studies the effect of admixture addition on the strength characteristics of solidified engineering waste slurry, so the change in water content of the slurry caused by the admixtures is not considered.

Before preparing the strength samples, clean the sample mold (cube with a side length of 70.7 mm) and dry it. Then, evenly apply vaseline on the inner walls and bottom to reduce friction between the sample and the mold, and weigh and record the mass of the mold. Add the target mass of cement to the "sludge + bentonite" mixture and stir again evenly. Fill the stirred mixture into the sample mold in 3-4 batches, vibrating it multiple times during the process to eliminate bubbles and ensure uniform and dense samples [24]. After filling the mold, use a soil scraper to level the sample surface and place it in a standard curing chamber for curing. After 1-2 days of curing, when the sample has formed, demold the sample. Then, continue curing samples that have not reached the target curing age until they do. The specific experimental scheme is shown in Table 3. End the test when the soil sample's stress-strain curve reaches a peak value, or when the soil sample's strain exceeds 15%, and take the peak stress or the stress corresponding to an axial strain of $\varepsilon = 15\%$ as the soil sample's unconfined compressive strength [25]. Additionally, the entire experiment should be completed within 8-10 minutes.

For the scanning electron microscope (SEM) test, samples of cement at a 28-day curing age and with a 25% cement dosage, including specimens with 9% bentonite and without bentonite, were selected to observe the micro-differences at a magnification of one thousand times. The SEM test specimens were all taken

Table 1. Basic physical properties of experimental soil.

Water content (%)	Dry density (g/cm^3)	Specific gravity of soil particle	Liquid limit (%)	Plastic limit (%)	Organic content (%)
52.26	1.38	2.17	37.71	22.06	3.2

Table 2. Chemical composition of experimental bentonite.

SiO_2	Al_2O_3	MgO	Na_2O	CaO	K_2O	Fe_2O_3	TiO_2	Li_2O	Ignition loss
68.89	12.91	3.27	2.16	1.91	0.68	1.95	0.33	0.76	6.81

Table 3. Mixture proportion design of test specimens.

Water content	Cement ratio	Curing time	Bentonite content
(%)	(%)	(day)	(%)
25	6	7	0
25	12	28	3
25	18	90	6
25	25	--	9
25	--	--	12

from the cross-sections that were relatively flat after the failure of the unconfined compressive strength test. Due to the poor conductivity of the soil samples, they were first gold-sputtered before being placed in the SEM vacuum chamber for testing [26].

Results and Discussion

Strength

Fig. 1 shows the relationship between the unconfined compressive strength and the amount of bentonite added under different curing ages and cement contents. At the same curing age, the unconfined compressive strength of waste sludge increases first and then decreases with the increase of bentonite content. Compared to waste sludge without bentonite, the addition of bentonite increases the unconfined compressive strength of the soil. This is mainly because bentonite improves the rheological properties and shear strength of the samples, increases cohesion, and enhances the stability of the specimens [27]. Additionally, bentonite fills the internal pores of the samples and reacts chemically with sludge and cement to form cementing substances, which strengthens the bond between soil particles and further enhances the compressive strength of the specimens [28]. However, when the bentonite content is less than 3%, the unconfined compressive strength does not significantly increase. This is because, at lower bentonite and cement contents, excess water does not participate in the hydration reaction of cement, and the hydrophilic action of bentonite is not fully exerted [29]. This causes excess water to form free water retained between soil particles, limiting the strength improvement of the modified soil. Moreover, when the bentonite content exceeds 9%, excessive swelling of bentonite from water absorption overly fills the pores, causing internal micro-cracks in the soil, expelling gases (CO_2) from the pores, and consuming some free water [30]. These factors lead to

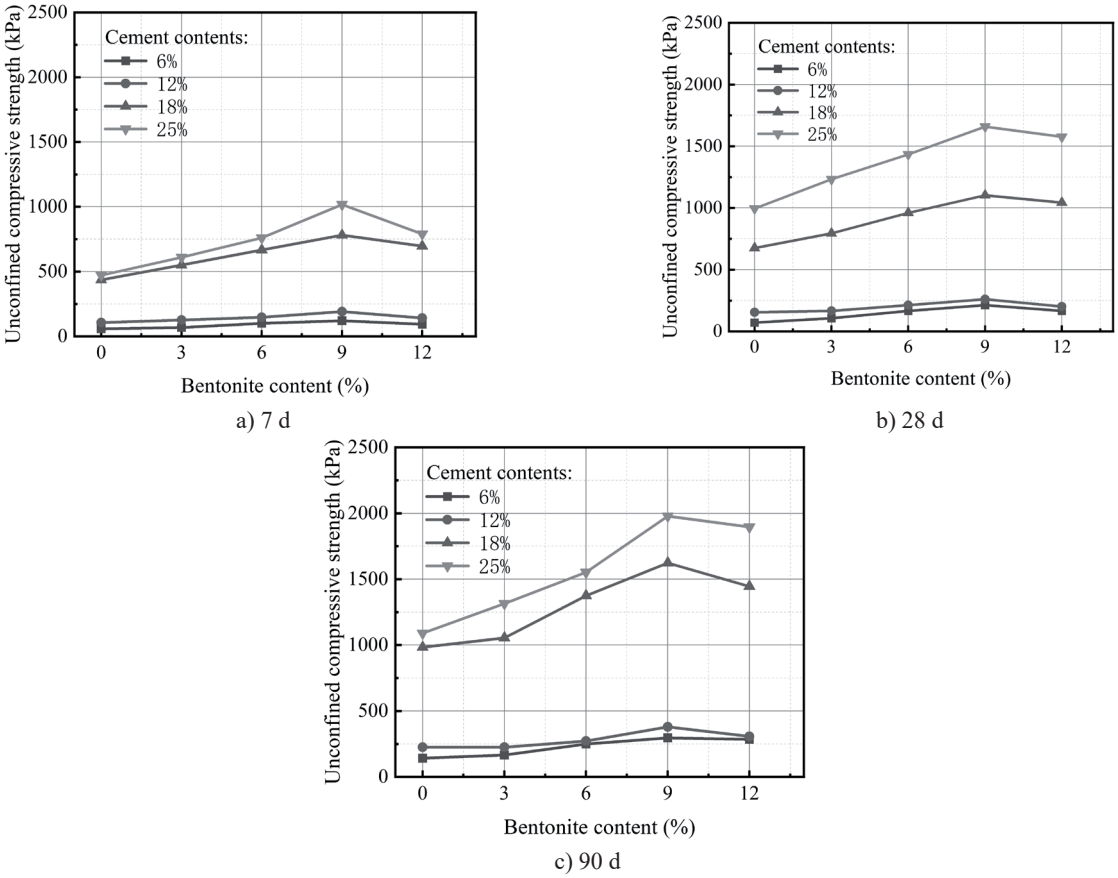

Fig. 1. Effect of bentonite content on strength.

uneven strength distribution in the sludge, even creating local weak points, thereby reducing the effectiveness of the unconfined compressive strength improvement and leading to unstable strength enhancement in the specimens.

To further study the effect of bentonite addition on the strength of waste sludge, the parameters Δq_u and $\Delta q_u/q_0$ are introduced for analysis. Here, q_0 is the unconfined compressive strength of waste sludge without bentonite at the same curing age, and q_u is the unconfined compressive strength of waste sludge with bentonite at different curing ages; Δq_u (= $q_u - q_0$) is the difference in unconfined compressive strength between waste sludge with and without bentonite at the same curing age.

The effects of bentonite content and curing time on the unconfined compressive strength (UCS) development of stabilized waste sludge are summarized in Table 4. The results indicate a clear enhancement in both the strength increment (Δq_u) and the relative strength increment ratio ($\Delta q_u/q_0$) with increasing bentonite content. Specifically, at a curing time of 90 days, Δq_u increased from 94.78 kPa to 473.92 kPa as the bentonite content rose from 3% to 12%, while$\Delta q_u/q_0$ improved from 12.12% to 60.61%. This trend underscores the significant role of bentonite in improving the mechanical performance of cement-stabilized sludge. Moreover, the strength enhancement is particularly notable at early curing ages. At 7 days, $\Delta q_u/q_0$ reached a peak of 70.40%, suggesting that bentonite contributes to rapid early strength development, likely due to its high water absorption capacity and interaction with cement hydration products. However, the marginal benefit of increasing bentonite content diminishes over time. At 90 days, the $\Delta q_u/q_0$ corresponding to 12% bentonite content was only slightly higher than that of 9%, and even exhibited a slight decline in efficiency. This suggests a possible threshold beyond which excess bentonite may adversely affect the microstructure. Excessive bentonite can disrupt the compact arrangement of soil particles, leading to irregular fabric and stress concentration zones that weaken the overall strength.

Therefore, based on both strength magnitude and efficiency, a bentonite content of 9% is identified as the optimal dosage for the specific waste sludge tested in this study. It balances structural enhancement and material efficiency, yielding a UCS of 639.81 kPa and a relative gain of 48.92% after 90 days of curing.

Failure Strain

The failure strain is the strain that occurs when a specimen reaches its strength limit, and it can be used to assess the load-bearing capacity and safety of materials [31]. It is significant for understanding the behavior and lifespan of materials under long-term use and exposure to different environmental conditions. Fig. 2 shows the failure strain of waste sludge at different curing ages and with different bentonite contents. At the same curing age, the addition of bentonite causes an increase in the failure strain of the specimen, reducing the brittleness of the soil, and better meeting the requirements for the deformation characteristics of cured soil in engineering applications like embankments or foundations. It is noteworthy that the maximum failure strain occurs at a bentonite content of 9%. This is because the unconfined compressive strength is highest when the bentonite content is 9%, leading to an increase in the time to failure and, consequently, an increase in the failure strain.

At the same bentonite content, the failure strain of the specimens decreases from the early age (7 days) to the mid-age (28 days). This is because the strength of the specimens is relatively low at the initial age. Therefore, when the specimens are subjected to external loads or stress, they tend to undergo larger deformation and failure, leading to a higher failure strain. The failure strain of the specimens from the mid-age (28 days) to the later age (90 days) only slightly decreases or remains unchanged. The reason for this phenomenon is that after the mid-age, the hydration reaction of the cement gradually stabilizes, and the rate of strength increase slows down [32].

In the early age of the specimens, there is usually a higher initial strain (elastic strain). This is because, at the time when the load is first applied, the microstructure between the cement particles and the cementitious materials has not yet fully developed and is still in a relatively loose state. At this stage, failure strain typically does not occur. As the age of the specimens increases, the cement paste gradually solidifies and hardens, and the microstructure of the specimens becomes more compact and stable. This leads to a gradual decrease in the initial strain of the specimens, and the failure strain starts to gradually increase. In the later age of the specimens, as time progresses, the microstructure

Table 4. Δq_u and $\Delta q_u/q_0$ of waste sludge with different bentonite contents.

Cement ratio (%)	Curing age (day)	Δq_u (kPa)				$\Delta q_u/q_0$ (%)			
		Bentonite content (%)				Bentonite content (%)			
		3	6	9	12	3	6	9	12
15	7	115.56	219.24	287.37	225.20	36.13	68.54	89.84	70.40
	28	118.48	236.97	414.69	284.36	23.26	46.51	81.40	55.81
	90	94.78	379.14	639.81	473.92	12.12	48.49	81.82	60.61

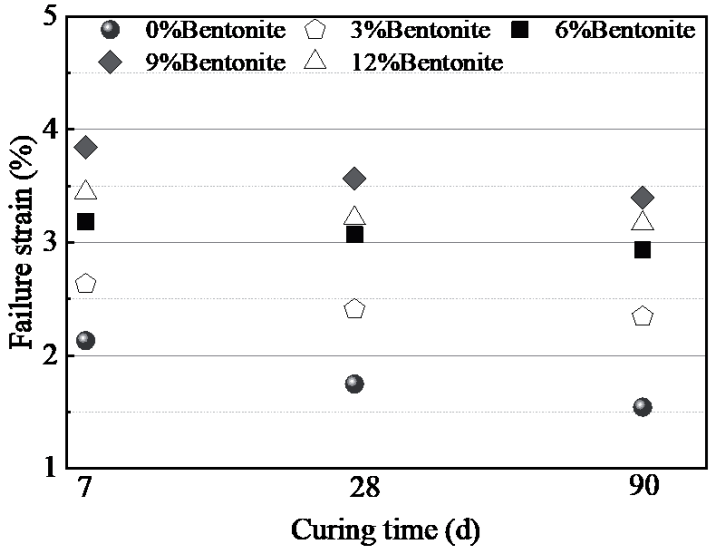

Fig. 2. Relationship between failure strain and curing age.

of the specimens further develops and matures. When the limit failure strain is reached, the specimens will no longer be able to withstand greater stress and will fail.

Deformation Coefficient

The deformation coefficient E_{50} can be obtained by dividing the stress corresponding to half the failure strain by half of the failure strain value, based on the stress-strain curve of the unconfined compressive strength test. Fig. 3 shows the relationship between the deformation coefficient and compressive strength. From the figure, it is evident that the strain value during the failure phase is usually greater than E_{50}, as the material has already approached or reached its limit state. E_{50} generally varies linearly with the unconfined compressive strength, consistent with the findings of Kang and Song et al. [33]. Through a literature review [34], the relationship between the compressive strength of the specimens studied in this paper and E_{50} can be found within the range shown in Fig. 3. Due to factors

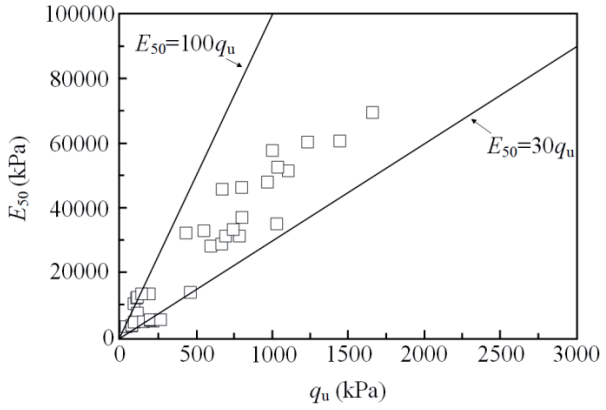

Fig. 3. Relationship between E_{50} and compressive strength.

such as the composition, mix ratio, pore structure, age, and loading conditions of the materials at different curing ages, the relationship between the strength of soil cured with accelerators and E_{50} is not certain. However, the range given in Fig. 3 can still be used for approximate prediction of E_{50} for engineering waste slurry cured with calcium-based accelerators.

In summary, the relationship between E_{50} and compressive strength can be summarized as follows: When the specimen has not yet fully exerted its maximum compressive strength, the E_{50} value is relatively low. As the compressive strength of the specimen increases, the value of E_{50} also increases accordingly. However, the specific relationship between E_{50} value and compressive strength is still influenced by a combination of factors, including the composition of the material, mix ratio, pore structure, age, and loading conditions.

Energy Consumption and Carbon Emission

To demonstrate that the incorporation of bentonite can replace part of the cement to enhance the mechanical properties of composites, four control groups were specifically selected. The specific details of the control

Table 5. The ratio table of the control group in the study of the mechanical properties of composites.

Group	Bentonite content	Cement content
--	(%)	(%)
A	0	12
B	9	6
C	0	25
D	9	18

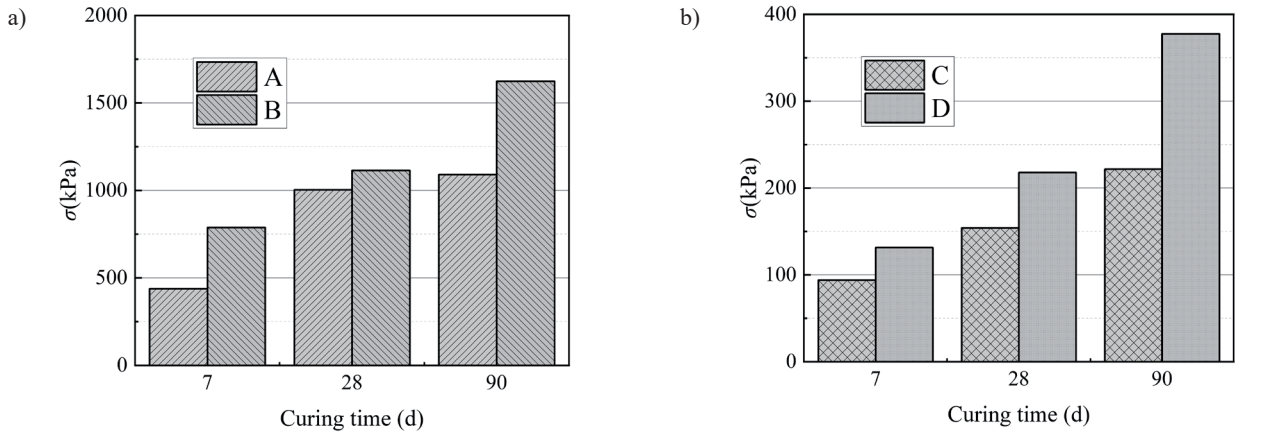

Fig. 4. Bentonite substitute cement experimental control results.

groups are shown in Table 5. The comparison results are illustrated in Fig. 4.

This study assesses the impact of substituting bentonite for cement on the mechanical properties of composite materials by setting up four control groups (Groups A, B, C, and D). Group A (0% bentonite, 12% cement) and Group C (0% bentonite, 25% cement) serve as baselines, while Group B (9% bentonite, 6% cement) and Group D (9% bentonite, 18% cement) are compared with Groups A and C, respectively. The research found that under different curing time conditions, samples from Groups B and D exhibited superior mechanical performance compared to Groups A and C. This finding suggests that the addition of bentonite, while reducing cement usage, did not diminish the mechanical performance of the composite material, but rather enhanced it. Notably, Group B, compared to Group A, reduced cement usage by 50% while maintaining the same volume, and the comparison between Groups C and D showed that the addition of bentonite reduced cement usage by about 30%. This result reveals the potential of bentonite as an alternative material in improving the mechanical performance of composite materials. Further analysis indicates that using bentonite to replace some of the cement is beneficial not only in terms of material performance but also significantly in environmental protection and sustainable development. According to related studies, the production of one ton of cement clinker requires approximately 1.7 tons of clay and 850,000 kilocalories of energy, while emitting about 0.94 tons of carbon dioxide. In contrast, the production process of bentonite consumes much less energy and has lower carbon emissions. For example, in engineering projects with a 25% cement blend, replacing it with 18% cement and 9% bentonite can reduce cement usage by about 30%. This substitution method can save about 200,000 kilocalories of energy consumption and reduce carbon dioxide emissions by 0.16 tons per ton of cement soil. The use of bentonite reduces the demand for cement, thereby decreasing energy consumption and carbon emissions. This is particularly important in the current global context of energy crises and climate change. By reducing cement usage, we not only lower the energy consumption and carbon footprint in industrial production but also provide a practical path for the green transformation of the construction industry.

Permeability Characteristics

This paper takes the specimens with a curing age of 28 days and a cement content of 9% as an example, and describes the logarithmic permeability coefficient-cement content curve under different bentonite contents (Fig. 5). The permeability coefficient of the sample with 3% bentonite content decreases the most significantly. As the bentonite content continues to increase, the decrease in the permeability coefficient slows down. In bentonite, Al^{3+} and Si^{4+} can be replaced by Mg^{2+} and Ca^{2+} in cement, causing the exchanged cations to carry a residual negative charge [35]. Additionally, due to the weak binding between montmorillonites, bentonite can also absorb polar cations and water [36]. The greater the amount of bentonite added, the more negative charges, and the stronger the electrostatic attraction. The resultant thicker double layer also thickens the water film, increasing the number of adsorbed water molecules on the surface, thereby enhancing the expansiveness of the bentonite [37]. When bentonite fully contacts water, the exchanged cations and the water molecules at the bottom of the crystal cell can hydrate, leading to the expansion of bentonite. The expansion of bentonite fills the small pores in the soil, including those between soil particles, cement particles, and aggregates, thereby reducing the permeability coefficient and lowering the permeability. When the bentonite content is too high, it leads to an increase in soil saturation, and the newly added bentonite cannot effectively fill the saturated pores, slowing down the change in the permeability coefficient. Moreover, an excessive amount of bentonite changes the pore structure of the soil, creating a denser pore structure, increasing the resistance of water movement in the soil, and thereby slowing down the permeation rate. At the same time, the small particle

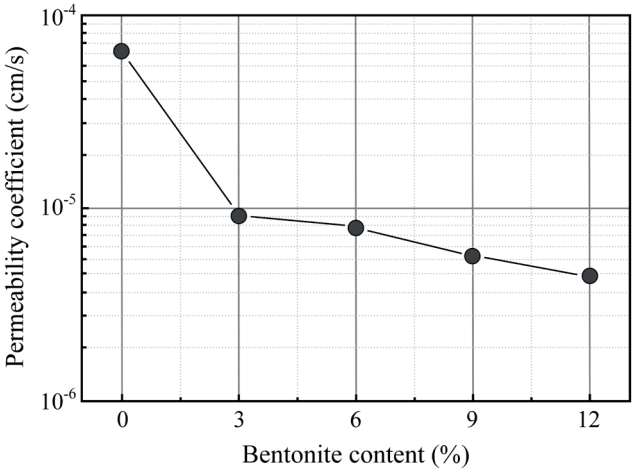

Fig. 5. Relationship between permeability coefficient and bentonite content.

size of bentonite, when added in excess, may clog the pores in the soil, reducing the pathways for water to pass through the soil, resulting in a slower decrease in the permeability coefficient. Therefore, these factors collectively lead to a slowdown in the decrease of the permeability coefficient when the bentonite content is too high.

Calculation of Strain Energy

The strain energy can be divided into three types, i.e., U, which denotes the total energy absorbed by the sample; U_e, which represents the elastic strain energy stored in the sample; U_d, the dissipated energy that is responsible for the plastic deformation and crack propagation. The three types of energy can be expressed as follows [38]:

$$U = U_e + U_d \tag{1}$$

$$U = \int \sigma_1 \, \mathrm{d}\varepsilon_1 + 2\int \sigma_3 \, \mathrm{d}\varepsilon_3 + \frac{3(1-2\nu_0)}{2E_0}(\sigma_3^0)^2 \tag{2}$$

$$U_\mathrm{e} = \frac{1}{2E_\mathrm{u}}[\sigma_1^2 + 2\sigma_3^2 - 2\upsilon_\mathrm{u}(\sigma_1^2 + 2\sigma_1\sigma_3)] \tag{3}$$

where E_0, E_u, ν_0, and ν_u are the initial elasticity modulus, unloading elastic modulus, initial Poisson's ratio, and the unloading Poisson's ratio, respectively. σ_1 is the major principal stress, σ_3 is confining pressure, ε_1 is axial strain, and ε_3 is lateral strain.

Take the sample with bentonite content of 9%, cement content of 18% and curing age of 90 days as an example, U, U_e, and U_d of the sample are shown in Fig. 6. During the initial compressive and linear-elastic deformation phases, the energy behavior of the sample was primarily consistent with energy accumulation and energy hardening; thus, most of the total energy was converted to elastic energy being stored in the sample. Thereafter, the total energy curve began to diverge from the elastic energy curve as the sample entered the elastic–plastic deformation phase. When the sample reached its peak strength, the elastic energy was released, and the dissipated energy increased rapidly due to the macroscopic damage of the sample. The energy absorbed by the sample in the post-peak phase was dissipated completely, which led to further expansion of the cracks.

Microstructure

The SEM results provide detailed observation of the microstructure and composition of the specimen samples. Fig. 7 shows the micro-differences under SEM between the specimens with and without bentonite added, at a 28-day curing age and with a 25% cement content. From the figure, it can be seen that the samples without added bentonite are mainly composed of hydration products and cement particles. In Fig. 7b),

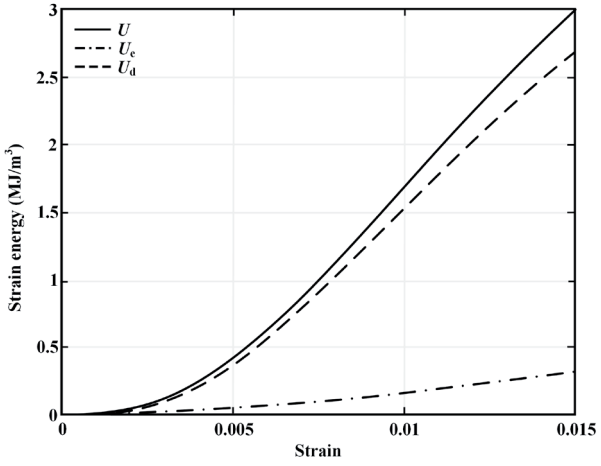

Fig. 6. Strain energy evolution curves and crack volumetric evolution curve.

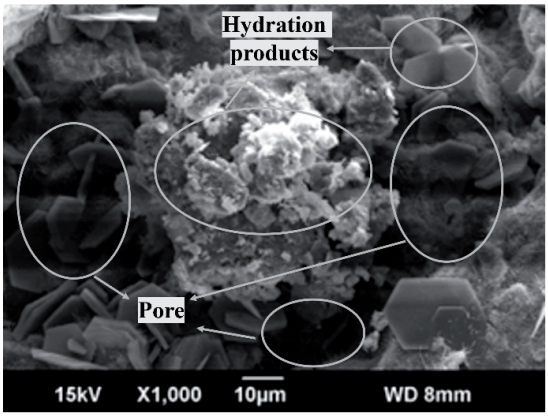

a) bentonite content 0%

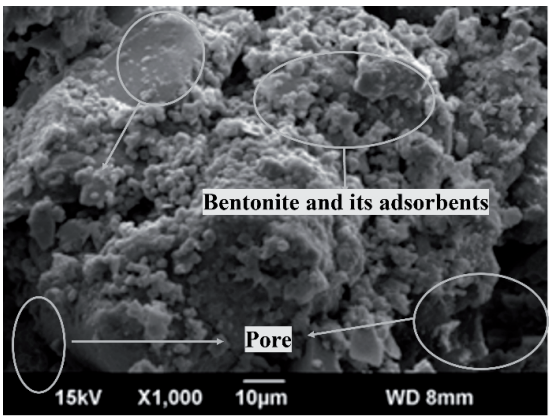

b) bentonite content 9%

Fig. 7. Effect of bentonite on the microscopic morphology of test specimens.

there is an interaction between bentonite particles and hydration products, specifically manifested as physical connections or chemical reactions between particles, leading to particle aggregation or the formation of complex network structures.

The addition of bentonite particles fills the micro-pores in the specimens. Due to the small size of bentonite particles, they can enter finer pore spaces and fill the pores in the soil. This helps to reduce the porosity of the specimens and increase the compactness of the soil. Additionally, bentonite particles have adsorptive properties, allowing them to adsorb water and other solute substances. When bentonite particles fill the pores, they form an adsorption layer that adsorbs and fixes water and solutes in the soil, thereby altering the soil's moisture characteristics and chemical properties. In the specimens mixed with bentonite, bentonite particles may exhibit some specific crystalline features [39]. Through SEM observation, the micro-crystalline structure on the surface of bentonite particles or the crystalline connections between particles can be observed. These crystalline features can further reflect the interaction between bentonite and the cement matrix.

Engineering Case

Project Overview

The engineering project underpinning this study is a subway tunnel project in a water-rich, weak stratum. The specific stratification is as follows: miscellaneous fill layer, clay layer, silty clay layer, silty clay layer, silt mixed with silty sand, silty clay layer, silty clay layer. Most sections of this project's route are shallow and covered with thick layers of silt or silty sand. Under dynamic water pressure, these types of soils are prone to liquefaction or piping, which has a significant negative impact on the tunnel shield construction. During construction, adverse geological phenomena such as gushing water, quicksand, and collapse are prone to occur. In this interval, it's crucial to reinforce a certain range of soil around the shield tunnel excavation, which generally consists of soft cohesive soil with poor self-stabilization or highly permeable silty and sandy soil, to enhance the soil strength and reduce the permeability coefficient.

Field Test

In the subway section, the triaxial mixing construction process was used, and drilling and coring were conducted 28 days after the completion of the construction. The photos of the cores obtained (Fig. 8) show good coherence and exhibit the typical color of specimens. In the laboratory, the collected core-shaped samples were cut and polished to create specimens with a height-to-width ratio of 1:1. Unconfined compressive strength tests and permeability tests were then carried out on these specimens.

According to the unconfined compressive strength tests, the compressive strength at various depths is determined, with the test results shown in Fig. 9a). The results show that the unconfined compressive strength of core samples from weakly reinforced areas is generally concentrated between 0.6 and 1 MPa; while

Fig. 8. Pictures of drilling and coring.

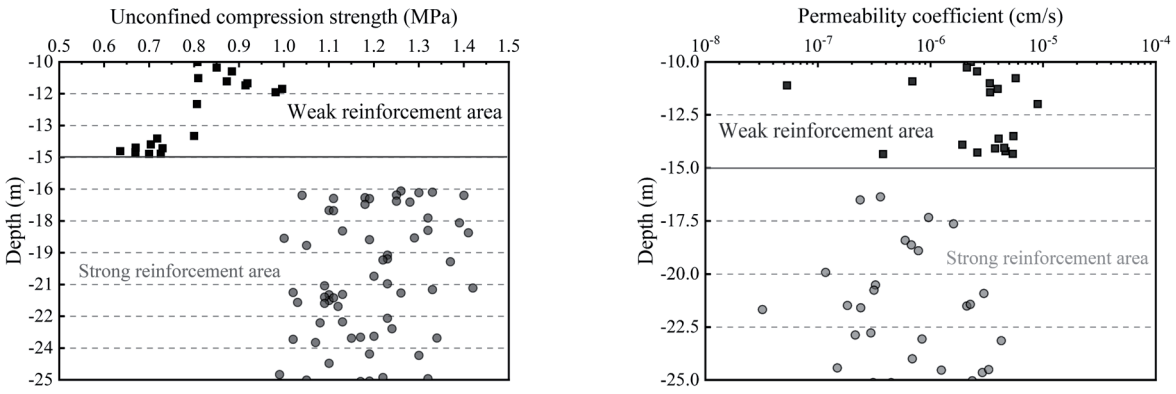

a) Strength test b) Penetration test

Fig. 9. Results of drilling sampling test in the strong reinforcement area.

in strongly reinforced areas, the unconfined compressive strength of the core samples is all above 1 MPa, with the maximum value reaching 1.48 MPa. However, some core samples show anomalous strengths. This is due to uneven mixing in some local areas during the triaxial mixing construction of the specimens, resulting in the formation of cement-rich clinker and soil blocks with less cement. Field sampling results indicate that the strength of the soil layers does not decrease with increasing depth. This paper identifies two primary reasons for this phenomenon: the low average cutting line speed of the mixing piles results in weak mixing capabilities, causing the strength of soil layers to decrease gradually with depth; additionally, the lower strength of the lower soil layers contributes to reduced sampling strength.

Fig. 9b) shows the permeability coefficient test results of core samples from the project site. The results indicate that the permeability coefficients of the core samples are mostly in the order of 10^{-6} cm/s, with the lowest permeability coefficient reaching 3.27×10^{-8} cm/s. In silty sand and silty soil, the permeability coefficients of the core samples are generally below 10^{-7} cm/s, indicating good impermeability. Considering the damage to the samples during sampling and transportation, the actual permeability coefficient may be even lower, meeting the impermeability requirements. Additionally, the impermeability of core samples from deeper soil layers is better than that from upper layers, a phenomenon similar to the results of the unconfined compressive strength test of the core samples. However, there are significant variations in permeability coefficients in some soil layers, mainly due to two reasons: First, uneven mixing during construction is inevitable, preventing the soil and cement slurry from forming a cohesive whole. In areas with uneven mixing, water channels can easily form near cement blocks, leading to large variations in permeability coefficients. Second, the sampling and transportation process can cause significant disturbance to the core, leading to micro-cracks within it, thereby greatly affecting the results of the permeability tests of the core.

Conclusions

To effectively encapsulate the comprehensive outcomes of this research, we have delineated four critical conclusions that collectively demonstrate the transformative effects of bentonite on waste sludge properties and their practical applications in engineering contexts. These conclusions not only underline the nuanced interplay between bentonite content and soil characteristics but also showcase the tangible impact of these modifications in a real-world engineering project, thereby bridging the gap between theoretical research and practical implementation.

(1) The unconfined compressive strength of waste sludge increases with the addition of bentonite, followed by a decrease as the bentonite content continues to increase. The strength enhancement is attributed to improved rheological properties, increased cohesion, and better soil particle bonding due to bentonite. However, at bentonite contents below 3%, there is no significant increase in strength, and above 9%, excessive swelling of bentonite can lead to uneven strength distribution and internal micro-cracks.

(2) The addition of bentonite causes an increase in the failure strain of the specimen, reducing soil brittleness. This enhancement is particularly noticeable at a bentonite content of 9%, where the maximum failure strain is observed. The failure strain decreases from the early curing age (7 days) to mid-age (28 days) due to the lower strength of the specimens at initial ages, and remains relatively stable or slightly decreases from mid-age to later age (90 days).

(3) The deformation coefficient E_{50} shows a linear variation with the unconfined compressive strength. When the specimen has not reached its maximum compressive strength, the E_{50} value is relatively low. As the compressive strength increases, the E_{50} value also increases. This relationship, however, is influenced by various factors, including material composition, mix ratio, pore structure, age, and loading conditions.

(4) The permeability coefficient shows a significant decrease with the addition of 3% bentonite and

slows down as the bentonite content increases. This decrease is attributed to the expansion of bentonite filling soil pores, thereby reducing permeability. High bentonite content can lead to increased soil saturation and a denser pore structure, which slows down the permeation rate and decreases in permeability coefficient.

Acknowledgements

The research presented here is supported by the National Key Research and Development Program of China (2023YFC3707801), National Natural Science Foundation of China (52478352), Natural Science Foundation of Jiangsu Province for Excellent Young Scholars (BK20211597), Bureau of Geology and Mineral Exploration of Jiangsu (2023KY06).

Conflict of Interest

The authors declare no conflict of interest.

References

1. LIU W., LIANG J., XU T. Tunnelling-induced ground deformation subjected to the behavior of tail grouting materials. Tunnelling and Underground Space Technology. **140**, 105253, **2023**.
2. PEI Q.-Y., ZOU W.-L., HAN Z., WANG X.-Q., XIA X.-L. Compression behaviors of a freeze – thaw impacted clay under saturated and unsaturated conditions. Acta Geotechnica. **19** (7), 4485, **2024**.
3. WU F., HU M. Influence of Carbon Dioxide on Micro-cracking in Calcite: An Atomistic Scale Investigation. Journal of Geophysical Research: Solid Earth. **130** (4), e2024JB030896, **2025**.
4. GU F., XIE J., VUYE C., WU Y., ZHANG J. Synthesis of geopolymer using alkaline activation of building-related construction and demolition wastes. Journal of Cleaner Production. **420**, 138335, **2023**.
5. TANG X., HU M. A reactive-chemo-mechanical model for weak acid-assisted cavity expansion in carbonate rocks. Rock Mechanics and Rock Engineering. **56** (1), 515, **2023**.
6. TANG Q., TIAN A., LING C., HUANG Y., GU F. Physical and mechanical properties of recycled aggregates modified by microbially induced calcium carbonate precipitation. Journal of Cleaner Production. **382**, 135409, **2023**.
7. TANG Q., ZHANG Y., GAO Y., GU F. Use of cement-chelated, solidified, municipal solid waste incinerator (MSWI) fly ash for pavement material: mechanical and environmental evaluations. Canadian Geotechnical Journal. **54** (11), 1553, **2017**.
8. GRONBA-CHYŁA A., GENEROWICZ A., KRAMEK A. Using Selected Types of Waste to Produce New Light Ceramic Material. Polish Journal of Environmental Studies. **30** (3), 2073, **2021**.
9. GRONBA-CHYŁA A., GENEROWICZ A. Municipal waste fraction below 10 mm and possibility of its use in ceramic building materials. Przemysl Chemiczny. **99** (9), 1318, **2020**.
10. TANG X., HU M. On the resilience of bio-cemented silica sands in chemically reactive environment. Geomechanics for Energy and the Environment. **37**, 100527, **2024**.
11. XIE J., LI C., LI B., TANG J., GU F. Thermal-alkaline activation enhances the mechanical properties of low-activity recycled concrete powder-derived geopolymers. Construction and Building Materials. **463**, 140020, **2025**.
12. CHEN Y., TIAN A., LUO X., ZHOU Y., TANG Q., KAWASAKI S. The physical and mechanical properties of recycled aggregates strengthened by enzyme induced carbonate precipitation. Soils and Foundations. **63** (6), 101394, **2023**.
13. TANG Q., SHI S., CHEN J., XU Q., LUO X. Modeling the influence of microbial growth on the hydraulic properties of porous media. Computers and Geotechnics. **147**, 104786, **2022**.
14. TABISH M., ZAHEER M.M., BAQI A. Effect of nano-silica on mechanical, microstructural and durability properties of cement-based materials: a review. Journal of Building Engineering. **65**, 105676, **2023**.
15. XIE J., ZHANG J., CAO Z., BLOM J., VUYE C., GU F. Feasibility of using building-related construction and demolition waste-derived geopolymer for subgrade soil stabilization. Journal of Cleaner Production. **450**, 142001, **2024**.
16. HARRAN R., TERZIS D., LALOUI L. Mechanics, modeling, and upscaling of biocemented soils: a review of breakthroughs and challenges. International Journal of Geomechanics. **23** (9), 03123004, **2023**.
17. TIAN A., TANG X., CHEN J., HU M. AC-assisted microbially induced carbonate precipitation for sand reinforcement: An experimental study. Geomechanics for Energy and the Environment. **40**, 100609, **2024**.
18. TRÜMER A., LUDWIG H.-M., SCHELLHORN M., DIEDEL R. Effect of a calcined westerwald bentonite as supplementary cementitious material on the long-term performance of concrete. Applied Clay Science. **168**, 36, **2019**.
19. TIRONI A., TREZZA M., IRASSAR E., SCIAN A. Activación térmica de bentonitas para su utilización como puzolanas. Revista De La Construcción. **11** (1), 44, **2012**.
20. LAIDANI Z.E.-A., BENABED B., ABOUSNINA R., GUEDDOUDA M.K., KADRI E.-H. Experimental investigation on effects of calcined bentonite on fresh, strength and durability properties of sustainable self-compacting concrete. Construction and Building Materials. **230**, 117062, **2020**.
21. HUANG Y. Influence of calcium bentonite addition on the compressive strength, efflorescence extent and drying shrinkage of fly-ash based geopolymer mortar. Transactions of the Indian Ceramic Society. **79** (2), 77, **2020**.
22. CHEW S.H., KAMRUZZAMAN A.H.M., LEE F.H. Physicochemical and engineering behavior of cement treated clays. Journal of Geotechnical and Geoenvironmental Engineering. **130** (7), 696, **2004**.
23. LI X., MA C., LYU J., HE M., WANG J., WANG Q., WANG Z., YOU X., LI L. Influence and mechanism of alkali-modified sludge on coal water slurry properties. Environmental Science and Pollution Research. **30** (10), 27372, **2022**.
24. LANG L., LI F., CHEN B. Small-strain dynamic properties of silty clay stabilized by cement and fly ash. Construction and Building Materials. **237**, 117646, **2020**.

25. CAI Y.Q., GUO L., JARDINE R.J., YANG Z.X., WANG J. Stress–strain response of soft clay to traffic loading. Géotechnique. **67** (5), 446, **2017**.
26. HOSSAIN A.K.M.N.-U., SELA S.K., HASAN N., RAHMAN H., HASSAN M.N., ALAM S.M.M. Surface modification of naturally dyed jute fabric to ameliorate its multifunctional properties and electrical conductivity. Vacuum. **207**, 111612, **2023**.
27. FU X.-L., ZHUANG H., REDDY K.R., JIANG N.-J., DU Y.-J. Novel composite polymer-amended bentonite for environmental containment: Hydraulic conductivity, chemical compatibility, enhanced rheology and polymer stability. Construction and Building Materials. **378**, 131200, **2023**.
28. TANG Q., KATSUMI T., INUI T., LI Z. Influence of pH on the membrane behavior of bentonite amended fukakusa clay. Separation and Purification Technology. **141**, 132, **2015**.
29. VISSER J.H.M. Fundamentals of alkali-silica gel formation and swelling: condensation under influence of dissolved salts. Cement and Concrete Research. **105**, 18, **2018**.
30. REN P., LING T.-C., MO K.H. Recent advances in artificial aggregate production. Journal of Cleaner Production. **291**, 125215, **2021**.
31. ZHOU K., LEI D., CHUN P.-J., SHE Z., HE J., DU W., HONG M. Evaluation of BFRP strengthening and repairing effects on concrete beams using DIC and YOLO-v5 object detection algorithm. Construction and Building Materials. **411**, 134594, **2024**.
32. NTIMUGURA F., VINAI R., HARPER A., WALKER P. Mechanical, thermal, hygroscopic and acoustic properties of bio-aggregates – lime and alkali – activated insulating composite materials: a review of current status and prospects for miscanthus as an innovative resource in the south west of England. Sustainable Materials and Technologies. **26**, e00211, **2020**.
33. SONG M.-M., ZENG L.-L., HONG Z.-S. Pore fluid salinity effects on physicochemical-compressive behaviour of reconstituted marine clays. Applied Clay Science. **146**, 270, **2017**.
34. BALAGOSA J., YOON S., CHOO Y.W. Experimental investigation on small-strain dynamic properties and unconfined compressive strength of gyeongju compacted bentonite for nuclear waste repository. KSCE Journal of Civil Engineering. **24** (9), 2657, **2020**.
35. SUN Z., CHEN Y.-G., YE W.-M. A systematic review of bentonite/concrete interaction system in HLW disposal repositories: Theoretical, experimental and geochemical modelling analysis. Construction and Building Materials. **353**, 129075, **2022**.
36. TANG Q., KATSUMI T., INUI T., LI Z. Membrane behavior of bentonite-amended compacted clay. Soils and Foundations. **54** (3), 329, **2014**.
37. ALEKSEEVA O.V., NOSKOV A.V., AGAFONOV A.V. Structure, physicochemical properties, and adsorption performance of the ethyl cellulose/bentonite composite films. Cellulose. **29** (7), 3947, **2022**.
38. XIE H.-P., JU Y., LI L.-Y. Criteria for strength and structural failure of rocks based on energy dissipation and energy release principles. Yanshilixue Yu Gongcheng Xuebao/Chin. Journal of Rock Mechanics and Geotechnical Engineering. **24** (17), 3003, **2005**.
39. ALZAMEL M., FALL M., HARUNA S. Swelling ability and behaviour of bentonite-based materials for deep repository engineered barrier systems: influence of physical, chemical and thermal factors. Journal of Rock Mechanics and Geotechnical Engineering. **14** (3), 689, **2022**.